

24. Kantrowitz, A. J. *J. Chem. Phys.* 1951, 19, 1097.25. Frisch, H. L. *J. Chem. Phys.* 1957, 27, 90.26. Courtney, W. G. *J. Chem. Phys.* 1962, 36, 2009.27. Sridharan, R.; de Levie, R. J. *Electroanal. Chem.* 1984, 169, 59.

Effect of Mn-addition on Catalytic Activity of Mn/In₂O₃ in Methane Activation

Jong Sik Park, Jong Ho Jun[†], Yong Rok Kim, and Sung Han Lee*

Department of Chemistry, Yonsei University, Seoul 120-749, Korea

[†]*Department of Applied Chemistry, Konkuk University, Chungju 380-701, Korea*

Received July 11, 1994

Mn/In₂O₃ systems with a variety of Mn mol% were prepared to investigate the effect of Mn-addition on the catalytic activity of Mn/In₂O₃ in the oxidative coupling of methane. The oxidative coupling of methane was examined on pure In₂O₃ and Mn/In₂O₃ catalysts by cofeeding gaseous methane and oxygen under atmospheric pressure between 650 and 830 °C. Although pure In₂O₃ showed no C₂ selectivity, both the C₂ yield and the C₂ selectivity were increased by Mn-doping. The 5.1 mol% Mn-doped In₂O₃ catalyst showed the best C₂ yield of 2.6% with a selectivity of 19.1%. The electrical conductivities of pure and Mn-doped In₂O₃ systems were measured in the temperature range of 25 to 1000 °C at P_{O₂}'s of 1×10⁻⁷ to 1×10⁻¹ atm. The electrical conductivities were decreased with increasing Mn mol% and P_{O₂}, indicating the specimens to be n-type semiconductors. Electrons serve as the carriers and manganese can act as an electron acceptor in the specimens. Manganese ions doped in In₂O₃ inhibit the ionization of neutral interstitial indium or the transfer of lattice indium to interstitial sites and increase the formation of oxygen vacancy, giving rise to the increase of the concentration of active oxygen ion on the surface. It is suggested that the active oxygen species adsorbed on oxygen vacancies are responsible for the activation of methane.

Introduction

The conversion of CH₄ to C₂ hydrocarbon or to CO₂ is becoming important both for various technological applications and from a basic scientific point of view. Especially, the methane coupling reaction has become an active research area since Keller and Bhasin¹ reported the C₂ hydrocarbon production from methane over metal oxide catalyst in 1982. It has been known that high surface basicity of catalyst is required to achieve good C₂ hydrocarbon selectivity in the oxidative coupling of methane and alkali promoters can enhance the basicity of catalyst.^{2,3} The catalytic activities of metal oxides are closely linked to their nonstoichiometric composition and electronic properties. Ambigues and Teichner⁴ showed that correlations between the electrical conductivity and catalytic activity exist in metal oxide. Following their investigation of the conductivity effect of adsorbed oxygen on n-type zinc oxide, the catalytic effect on the other n-type and comparative results of p-type metal oxides led us to search for the correlations between oxide structure and catalytic activities. Therefore, it is believed that the study of catalytic activity of metal oxide in conjunction with its electrical properties is helpful to understand active sites and defects in the metal oxide. In the methane coupling reaction, a few results have been reported for the catalytic activity of metal oxide in relation to its electrical properties.

Indium sesquioxide has been known to be an n-type semiconductor and a nonstoichiometric compound with an In/O ratio larger than the ratio 2/3. Pure and impurity-doped indium sesquioxides find use in variety of applications such as electrodes in solar cells,⁵ fuel gas detectors,⁶ and heterogeneous oxidation-reduction catalysts.⁷ Otsuka *et al.*⁸ reported that In₂O_{3-x} showed an easy and reproducible redox cycle in the catalytic decomposition of water. Manganese atoms exist as multiple oxidation states in the oxide at high temperatures.⁹ It is expected that when Mn ions as impurity are doped into indium sesquioxide the oxide become either p-type or highly resistive n-type by self compensation effect in wide band gap semiconductors. In this work, Mn/In₂O₃ systems with a variety of Mn mol% were prepared to investigate the effect of Mn-addition on the catalytic activities of Mn/In₂O₃ systems in the oxidative coupling of methane. Methane conversions and C₂ selectivities of pure and Mn-doped In₂O₃ catalysts were investigated for the reaction and electrical conductivities of the catalysts were measured in the temperature range of 25 to 1000 °C at P_{O₂}'s of 1×10⁻⁷ to 1×10⁻¹ atm. XRD, XPS, SEM, DSC, and TGA techniques were used to investigate the structure and surface state of specimens. From the results, active sites on the surface and defects in the catalyst are discussed on the basis of solid-state chemistry.

Experimental Section

Mn/In₂O₃ catalysts were prepared from the mixture of In₂

*To whom correspondence should be addressed.

O₃ (99.99%, AESAR) and manganese carbonate by allowing direct solid state reaction. Manganese carbonate was prepared from the reaction of manganese nitrate solution with ammonium carbonate, followed by the precipitation. The precipitate was filtered and washed by deionized water and then dried at 100 °C in vacuum oven. Appropriate weights of MnCO₃ and In₂O₃ were well ground with an agate mortar and pestle. The mixture was put in a alumina boat, fired at 950 °C in flowing O₂ for 96 h, and then slowly cooled to room temperature at a rate of 50 °C/h. The amount of Mn incorporated in In₂O₃ was determined by atomic absorption spectrographic analysis and found to be 1.2, 2.5, 5.1 and 9.8 mol%, respectively. X-ray powder diffractometry for the samples was performed for identification of phase and structure. The XPS results of catalysts were achieved using VG ESCALAB with a high-pressure cell attached to the analytical vacuum chamber. The samples consisted of powdered catalysts compressed between a gold mesh and a gold foil to minimize charging effects and mounted on a transferable sample holder. The standard conditions for the analysis were: angle 45°; acquisition time 5 min.; pass energy 35.7 eV; Mg 400 W. The binding energies were corrected using 285.0 eV for the C(1s) level resulting from carbon as an internal standard. To get the information of a phase change in the specimens, differential scanning calorimetry and thermogravimetry analyses were performed. The results showed that phase change didn't occur in the present specimens in the temperature range of 25 to 1000 °C.

Kinetic studies were carried out in a conventional fixed-bed flow reactor operated at 1 atm. The reactor was an alumina tubing with 1.2 cm o.d and 30 cm length. The grain size of catalysts used in this work was 180-200 mesh and the BET surface areas of catalysts were in the range of 18.4 to 19.2 m²/g. The catalyst was held in the middle of the reactor and the section beyond the catalyst bed in the reactor was filled with alumina beads to reduce the free space. Following conditions were used to compare the activity of the catalysts: a 0.5 g sample loading of catalyst, a methane-to-oxygen feed mole ratio of 6 without a diluent gas, a feed flow rate at ambient conditions of 15 mL/min. The catalyst was pretreated at 450 °C in flowing O₂ for 6 hrs after loading into reactor. The range of reaction temperature explored was 650-830 °C. The purity of gaseous oxygen and methane was greater than 99.9%. The gaseous reactants were purified by passing over a bed of molecular sieve to remove water before introducing them into the reactor. Reaction products were analyzed by a HP5890 gas chromatograph equipped with a thermal conductivity detector and a quadruple mass spectrometer. Polapak Q column at 150 °C was used to analyze CO₂, C₂H₄, C₂H₆ and C₃ hydrocarbons, and molecular sieve 5A column at room temperature was employed to analyze O₂, CO and CH₄. The columns were connected in series through a 10-port Valco switching valve to isolate the molecular sieve 5A column while CO₂ and the hydrocarbons were eluted from the polapak Q column. Gas compositions were calculated using external standard gas mixture. Blank runs were performed over inert alumina beads in the absence of catalyst and approximately 2% conversion of methane to CO₂ was obtained in the reaction temperature range of 650 to 830 °C. The conversion of methane was calculated from the amounts of products generated and the methane introdu-

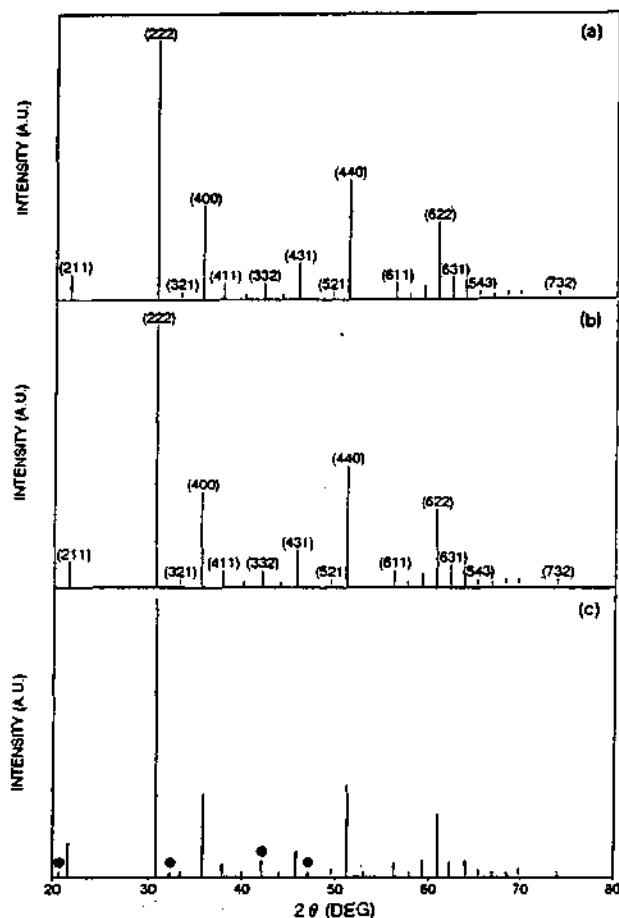


Figure 1. X-ray powder diffraction patterns of (a) pure In₂O₃, (b) 5.1 mol% Mn/In₂O₃ and (c) 9.8 mol% Mn/In₂O₃ catalysts (●: Mn₂O₃ phase).

ced in the feed stream. The selectivities were calculated on the basis of the conversion of methane to each product and the yield was obtained from the CH₄ conversion and selectivity to each product. The conversion of reactants and selectivities to products were typically compared after 2 h time-on-stream.

To measure the electrical conductivity, the powdered samples were made into pellets under a pressure of 1.2 tons/cm². The pellet was sintered in air at 1000 °C for 96 hrs and then cooled slowly to room temperature. After sintering, the sample was given a light abrasive polish on one surface, and then turned over and polished until the voids on both face of the specimen were fully eliminated. The sample was then cut into a rectangular shape and polished again. The dc conductivity was measured by means of the four-probe method described in the literature.¹⁰ The Po₂'s required were established using a mixture of O₂ in N₂. The conductivity was measured with increasing temperature at intervals of 50 °C and each measurement was made after the conductivity reached equilibrium.

Results

Figure 1 is the schematic X-ray diffraction patterns for various samples. 1.2, 2.5 and 5.1 mol% Mn/In₂O₃ specimens

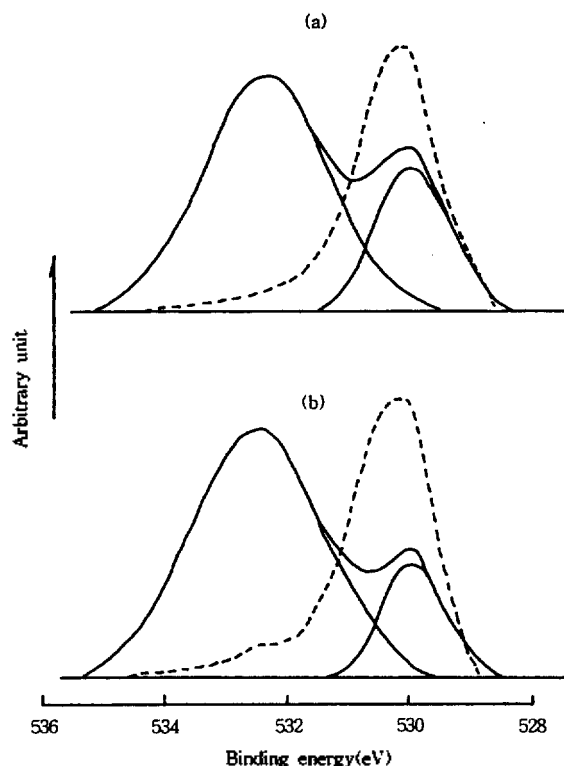


Figure 2. O(1s) spectra from (a) pure In_2O_3 and (b) 5.1 mol% $\text{Mn}/\text{In}_2\text{O}_3$. Dashed lines: after Ar^+ sputter cleaning; solid lines: after exposure in the mixture of O_2 and CH_4 at 650°C .

completely formed solid solutions, but Mn_3O_4 phase was detected in 9.8 mol% $\text{Mn}/\text{In}_2\text{O}_3$. The lattice parameters for the specimens obtained for the single phase bcc structure by the Nelson-Riley method and the values of the solid solution were not significantly changed from 10.11 \AA for pure In_2O_3 . We obtained the $\text{In}(2p)$ XPS spectra for pure In_2O_3 and 5.1 mol% Mn-doped In_2O_3 , in which indium metal peaks were not found. With an effective resolution of 1.0 eV and ± 0.2 eV precision, the binding energies of $\text{In}(3d_{5/2})$ for pure In_2O_3 and 5.1 mol% Mn-doped In_2O_3 were observed at 444.3 eV (FWHM 1.65 eV) and 444.8 eV (FWHM 1.62 eV), respectively, indicating the chemical shift by 0.5 eV to an upper position on binding energy. The $\text{Mn}(2p_{3/2})$ signal for 9.8 mol% $\text{Mn}/\text{In}_2\text{O}_3$ was observed at 641.2 eV (FWHM 2.36 eV) that was assigned in the literature to Mn_3O_4 .¹¹ Figure 2 shows the O(1s) XPS spectra for pure In_2O_3 and 5.1 mol% Mn-do-

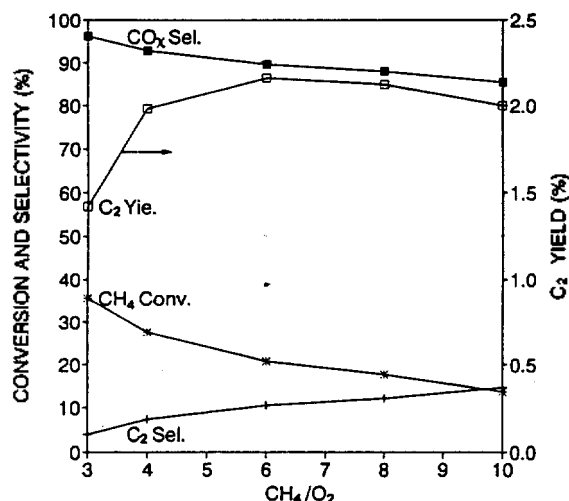


Figure 3. The effect of feed mole ratio of CH_4 and O_2 on product selectivities, conversion and yield over 2.5 mol% $\text{Mn}/\text{In}_2\text{O}_3$ catalyst (total feed flow rate = 15 mL/min, $T = 750^\circ\text{C}$).

ped In_2O_3 . Dashed lines indicate the spectra from the fresh catalysts after Ar^+ sputter cleaning. Solid lines indicate the spectra from the catalysts after exposure in the mixture of O_2 and CH_4 at 650°C for 30 min., in which two bands are observed near 530 and 532 eV, and their relative percentage changes with Mn-doping. Barr *et al.*¹² investigated the O(1s) XPS binding energies for the thin film of indium oxide produced on substrate through *d.c.* sputter deposition and observed two peaks at 530.3 eV due to the lattice oxygen and 531.9 eV due to the hydroxide. It is believed that the lower binding energy in Figure 2 arises from lattice oxygen (O_l) of the oxide and the higher binding energy is due to OH^- ions since carbonate form of indium does not exist even at room temperature.

In this work, the main products by the methane conversion reaction were H_2O , CO , CO_2 , C_2H_4 and C_2H_6 . Figure 3 shows the effect of methane-to-oxygen feed mole ratio on C_2 selectivity and C_2 yield. The best C_2 yield appeared at $n(\text{CH}_4)/n(\text{O}_2) = 6$. Results of activity and selectivities in the oxidative methane coupling reaction over various catalysts are given in Table 1. Pure In_2O_3 showed no C_2 selectivity. However, both the C_2 selectivity and the C_2 yield were increased by Mn-doping and the 5.1 mol% Mn-doped In_2O_3 catalyst showed the best C_2 yield of 2.6% with a selectivity of 19.1%. The C_2 selectivity and C_2 yield over 9.8 mol% $\text{Mn}/\text{In}_2\text{O}_3$ were

Table 1. Conversion and selectivity on pure In_2O_3 and $\text{Mn}/\text{In}_2\text{O}_3$ catalysts

Mn mol%	Conversion (%)		Selectivity (%)				C_2 Yield (%)	$\text{C}_2\text{H}_4/\text{C}_2\text{H}_6$
	CH_4	O_2	CO_2	CO	C_2H_4	C_2H_6		
0	37.7	95	45.7	53.8	0.2	0.4	0.2	0.5
1.2	12.7	90	41.4	53.0	1.9	3.7	0.7	0.5
2.5	12.8	80	43.9	41.1	5.4	9.8	2.0	0.6
5.1	13.8	80	45.5	35.4	6.7	12.4	2.6	0.5
9.8	14.0	80	46.7	43.3	5.5	4.5	1.4	1.2

Catalyst weight = 0.5 g, total feed flow rate = 15 cc/min, total pressure = 1 atm, CH_4/O_2 feed mole ratio = 6, and reaction temperature = 750°C .

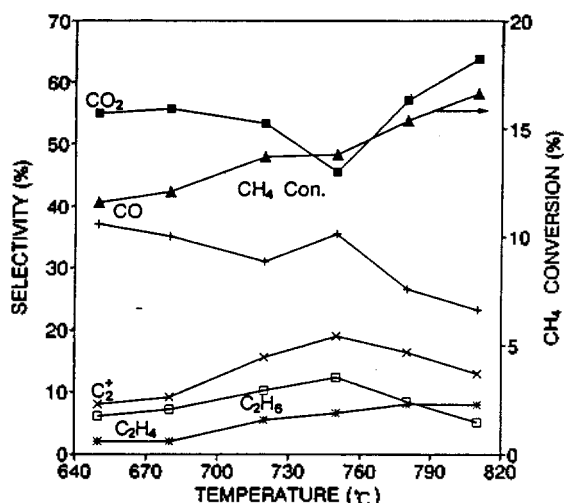


Figure 4. Variations of CH₄ conversion and product selectivities with temperature on 5.1 mol% Mn/In₂O₃ catalyst (total feed flow rate = 15 mL/min, $n(\text{CH}_4)/n(\text{O}_2)=6$).

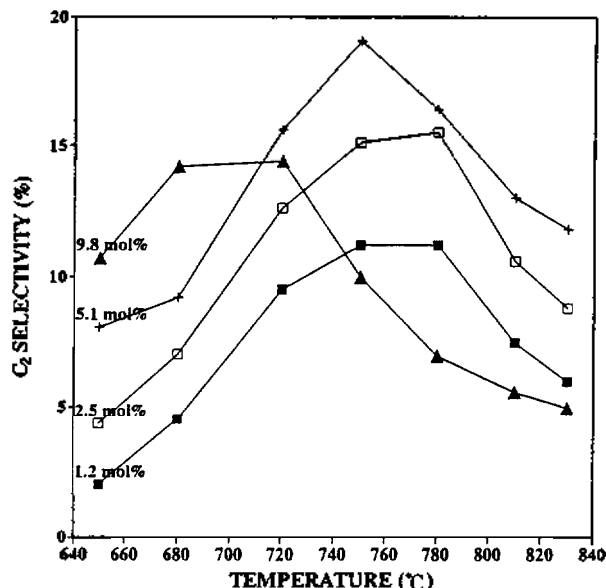


Figure 5. Variations of C₂ hydrocarbon selectivity with temperature on various Mn/In₂O₃ catalysts (total feed flow rate = 15 mL/min, $n(\text{CH}_4)/n(\text{O}_2)=6$).

lower than those over 5.1 mol% Mn/In₂O₃, which is believed to be resulted from some Mn₃O₄ phase existing on the surface. Figure 4 shows the temperature effects on CH₄ conversion and product selectivities over 5.1 mol% Mn/In₂O₃ catalyst. Figure 5 shows the temperature dependence of C₂ selectivity over various catalysts, in which the maximum C₂ selectivities appear around 750 °C over 1.2, 2.5, and 5.1 mol% Mn/In₂O₃ catalysts and at 700 °C over 9.8 mol% Mn/In₂O₃ catalyst.

Figure 6 shows log conductivity vs 1/T for pure In₂O₃ at various oxygen partial pressures from 10⁻⁷ to 10⁻¹ atm and temperatures from 25 to 1000 °C, in which conductivity peaks appear near 400 °C and diminish with decreasing P_{O₂}. Figure 7 shows log conductivity values plotted as a function of the

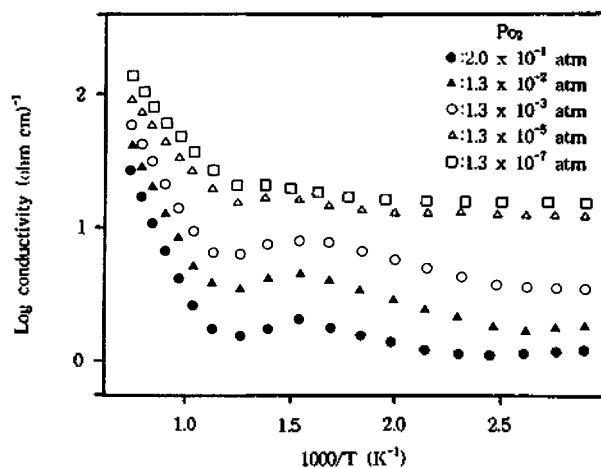


Figure 6. Log conductivity vs 1000/T for pure In₂O₃ at various P_{O₂}.

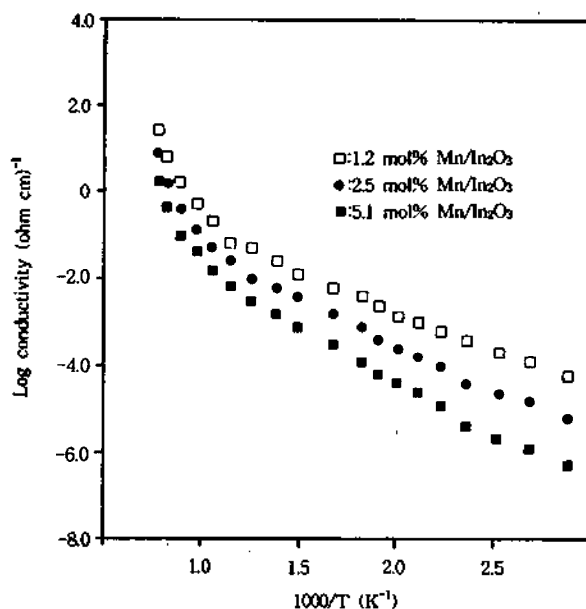


Figure 7. Log conductivity vs 1000/T at P_{O₂} = 2.0 × 10⁻¹ atm for various Mn/In₂O₃ catalysts.

reciprocal temperature for pure In₂O₃, 1.2, 2.5, and 5.1 mol% Mn-doped In₂O₃ catalysts in the temperature range of 25 to 1000 °C at P_{O₂} of 2 × 10⁻¹ atm. The curves were divided into high- and low-temperature regions. The electrical conductivity decreased as the amount of Mn increased. The activation energy, 1.36 eV, obtained for the high-temperature region between 600 and 1000 °C for pure In₂O₃, was in agreement with those (1.3–1.6 eV) of other investigators.^{13,14} Figure 8 shows isobaric conductivity plotted against 1/T for 5.1 mol% Mn-doped In₂O₃. The electrical conductivity decreased with increasing oxygen partial pressure, indicating the specimen to be n-type semiconductor.

Discussion

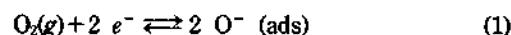
It has been known that the methane coupling on metal oxide is *via* the interaction of methane with active oxygen

species on the surface and involves the abstraction of a hydrogen atom from methane. When gaseous oxygen is chemisorbed on the surface of metal oxide, oxygen species can exist as forms of O_2^- , O_2^{2-} , O^- , and O_3^- . Superoxide (O_2^-) and peroxide (O_2^{2-}) species can be considered intermediates formed during oxygen dissociation and their existence mainly depends on the basicity of metal oxide and suitable sites for stability of the formed species. According to the FT-IR study of dioxygen adsorption on reduced cerium oxide by Onish *et al.*,¹⁵ superoxide species are formed immediately after O_2 introduction and successively converted into O_2^{2-} , O^- , and finally into O^{2-} (latt). Li *et al.*¹⁶ observed the existence of surface oxygen anions and surface coordinatively unsaturated oxygen (O^-) on the surface of well-outgassed CeO_2 from the FT-IR study of methane activation on cerium oxide. It has been reported that superoxide ions or ozonide ions act as stronger oxidant than peroxide ions in the oxidations of simple molecules such as H_2 , CO or CH_4 .¹⁷ Lunsford *et al.*^{18,19} confirmed the presence of O^- , O_2^- and O_3^- species from the ESR study of Li/MgO catalyst and found a strong correlation between the activity of the surface and the concentration of surface peroxide ions. According to the results of transient pulse and step-change experiments by Wolf *et al.*,²⁰ the O^- species are responsible for the C_2 hydrocarbon activity of Li/TiO₂ catalyst and lattice oxygen nonselectively activates methane. Petterson *et al.*²¹ studied the hydrogen abstraction from methane over pure and doped MgO crystal surface at multireference C1 levels by use of a cluster model combined with the surface Madelung potential, and proposed that Li and Na as dopants stabilize a reactive O^- state at the surface and give abstraction reactions with low energy barrier (4-6 kcal/mol). Although various models of methane activation in the oxidative coupling of methane have been proposed and the nature of the active species remains to be determined, it is generally accepted that the O^- species on the surface of oxide catalyst selectively activate methane in the reaction. When CH_4 reacts with active O^- species on the surface of metal oxide, methyl radical is generated and OH^- is simultaneously formed.

As shown in Table 1, pure In_2O_3 was a poor catalyst in the oxidative methane coupling, but active in deep oxidation of methane. However, the yield and selectivity of C_2 hydrocarbon product gradually increased with increasing Mn mol% and the yield reached a maximum for the catalyst with 5.1 mol% Mn-doping. Figure 2 shows the O(1s) XPS spectra quenched to room temperature after the reaction at 650 °C, in which the higher binding energy is arising from OH^- ions and the lower binding energy from lattice oxygens (O_l) as mentioned above. The relative percentage of the integrated intensity of the higher binding-energy species to the lower binding-energy species increased with increasing Mn mol%. In_2O_3 can react with H_2O and shows a catalytic activity in the decomposition of water.⁸ In this work, indium oxide can be converted into indium hydroxide since indium oxide reacts with H_2O producing during the reaction of O_2 and CH_4 . Therefore, it is believed that the peak at 532.1 eV for pure In_2O_3 after reaction corresponds to indium hydroxide, implying indium hydroxide to be the dominant phase on the surface of In_2O_3 catalyst. If the 5.1 mol% Mn-doped In_2O_3 catalyst contains a lot of active sites for methane on its surface, the intensity due to OH^- ions for the 5.1 mol% Mn-

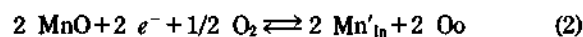
doped In_2O_3 catalyst will be higher than that for pure In_2O_3 catalyst as shown in Figure 2 since OH^- ions can be more produced on the surface by the reaction of methane with active sites. If active sites for the methane coupling reaction are produced by Mn-doping, then the C_2 selectivity will be increased as shown in Table 1. At the surface of catalyst, charge transfer to form a double layer can be interpreted in terms of a space charge due to distributed ions within the oxide catalyst. This charge transfer in catalyst is associated with mobile electrons, but the density of energy levels available at the band edge is so low that the electrons are spread a substantial distance into the catalyst and can be considered a space charge. The electrical and chemical characteristics of the catalyst are considerably affected by this space charge. The formation of the double layers donates or withdraws the charge to or from the bands of the catalyst, and the density of current carriers is changed by a considerable fraction. As a consequence of O_2 -chemisorption on the surface of catalyst, the double layer forming will decrease the density of electrons near the surface. This decrease will lower the energy of further chemisorption of neutral oxygen molecules. In spite of the space charge on the surface of catalyst, the reactivity of catalyst would be related to its electrical properties.

In_2O_3 is known to be an oxygen deficient n-type semiconductor, represented as In_2O_{3-x} .¹³ The results of Figure 6 and 8 show that electrical conductivities of the specimens increase with decreasing P_{O_2} , indicating the present specimens to be n-type semiconductors. When gaseous oxygen is chemisorbed on the surface, the electron concentration should be decreased because the chemisorbed O_2 dissipates conduction electron in In_2O_3 . The oxygen vacancy in In_2O_{3-x} can act as a donor and an adsorption site for oxygen molecule.⁸ If O_2 is adsorbed on an oxygen vacancy defect (V_{O-2e^-}), the electrical conductivity should decrease according to the equilibrium



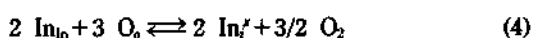
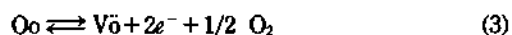
where e^- is a conduction electron trapped at an oxygen vacancy. The oxygen vacancy can become singly or doubly charged. The electrical conductivities of the present catalysts decreased with increasing oxygen partial pressure, indicating that electrons serve as the carriers. The curves of log conductivity vs $1/T$ of pure In_2O_3 at various oxygen partial pressures in Figure 6 show conductivity peaks near 400 °C, which is believed to be due to the chemisorption of O_2 . When O_2 -chemisorption occurs at any temperature, conductivity peak will appear because the concentration of conduction electron is decreased by the chemisorption of oxygen. Therefore, the appearance of conductivity peak in Figure 6 implies the existence of equilibrium (1) on the catalyst. The O^- ions should be primarily formed on the surface to activate methane. In Figure 7, the curves of log conductivity vs $1/T$ for various Mn-doped In_2O_3 catalysts are distinctly divided into high- and low-temperature regions. The electrical conductivity decreases as the amount of Mn-dopant increases, which means that Mn ions act as an electron acceptor in the specimen. Manganese forms very complex species with oxygen and a number of mixed valence compounds have been discovered in addition to simple oxides of Mn^{2+} , Mn^{3+} , and Mn^{4+} . According to the results of TPD and XRD for manganese oxide

by Burch *et al.*,²² when Mn₂O₃ or MnO₂ is heated in O₂ gas, Mn₃O₄ is formed as a stable phase of Mn oxide and all manganese ions in higher oxidation states can be reduced to Mn²⁺ by the reaction with CH₄. In this work, the Mn(2p_{3/2}) signal was observed at 641.2 eV and the binding energy is in good agreement with that for Mn₃O₄,¹¹ which indicates that Mn ions in Mn/In₂O₃ catalyst exist as a mixed state of Mn²⁺ and Mn³⁺. Since Mn²⁺ ions can act as an electron acceptor in In₂O₃, based on the principle of controlled valency, we can consider Eq. (2).

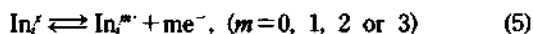


The concentration of conduction electron should be decreased with increasing the number of Mn²⁺ in In₂O₃ according to Eq. (2) and thus the electrical conductivity decreases with increasing Mn mol% as shown in Figure 7.

The predominant defects in indium sesquioxide are known to be oxygen vacancies at temperatures below 600 °C, whereas at temperatures above 600 °C, two different types of defects as electron donors were proposed: the Inⁱⁱ and the V_o model.¹³ In₂O₃ has a body centered cubic structure with 16 molecules per unit cell. One In³⁺ atom is surrounded by six equidistant oxygen atoms which lie approximately at the corners of a cube, with the two-body-diagonal opposite corners unoccupied, and the other In³⁺ atom is also surrounded by six oxygen atoms, but here two of the face-diagonal opposite corners are unoccupied. Thus, the lattice indium and lattice oxygen can easily diffused in the oxide, resulted in the formation of new donor level. Considering the formation of oxygen vacancy and interstitial indium as defects at higher temperatures, the defect equation may be respectively written as



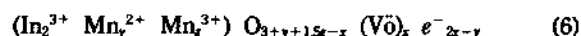
Eq. (3) generate the conduction electron. The neutral In_i' atoms formed by Eq. (4) may be successively ionized to singly charged, doubly charged or triply charged interstitial ions as in Eq. (5), resulted in the increase of concentration of conduction electron.



On the basis of the electroneutrality condition, the Po₂ dependence value of electrical conductivity for the V_o model and the Inⁱⁱ model are -1/6 and -3/16, respectively. Both values are consistent with the experimental data within experimental error, so it remains difficult to determine the predominant defect in the high-temperature region. In the high temperature region above 600 °C as shown in Figure 6, the electrical conductivity curve for pure In₂O₃ is typical of that for intrinsic conductivity. Wit *et al.*¹³ found that the mobility in the polycrystalline In₂O₃ was nearly constant in the temperature range from 25 to 700 °C. Therefore, it is believed that the change in conductivity is governed mainly by the change in carrier concentration so that the temperature dependence of the mobility can be neglected comparing to the temperature dependence of the carrier concentration. Since the donor levels in In₂O₃ are located around 0.01 eV just below the conduction band, electrons can be easily excited to the conduction band. It is believed that the activation

energy of In₂O₃, 1.36 eV, obtained in the high-temperature region at 2×10⁻¹ atm of Po₂ in Figure 7 consists of the energy for carrier migration, the energy for transfer of In_{In} atoms to an interstitial site, the energy for ionization of In_i to In_i^m, and the energy for the formation of oxygen vacancies. If Eq. (3) is predominant in In₂O₃ at higher temperatures, a high C₂ selectivity of pure In₂O₃ will be observed in the oxidative coupling of methane because a high concentration of active oxygen chemisorbed on oxygen vacancies is expected. However, pure In₂O₃ shows no C₂ selectivity in the oxidative coupling of methane at the reaction temperatures of 630-850 °C. The result implies that oxygen vacancies are not predominant in In₂O₃ at higher temperatures.

On the other hand, if interstitial indium ions are majority defect in indium sesquioxide at higher temperatures, the increase in C₂ selectivity by Mn-doping can be explained as follows. When small amounts of Mn²⁺ are doped into In₂O₃, Mn²⁺ can act as an electron acceptor and then the specimen can be described by



Eq. (6) means that electrons serve as the carriers. The electrons as carrier might be trapped in oxygen vacancies until the electrons obtain sufficient energy for excitation to the conduction band. In the 5.1 mol% Mn-doped In₂O₃ catalyst, activation energies for the electrical conduction, calculated in the high- and low-temperature region in Figure 7, are 1.45 and 0.43 eV at Po₂ of 10⁻¹ atm, respectively. The activation energy (0.43 eV) in the low-temperature region enables us to consider that electron carriers itinerate in the conduction band. The activation energy in the high-temperature region contains a contribution from the energy for the formation of the In_i which is in turn responsible for electrical conduction, as well as a contribution from the energy for migration. In the present catalysts, the electrical conductivity decreased with increasing Mn mol%. This result enable us to consider that the doped Mn inhibits the ionization of In_i' to In_i or the transfer of lattice indium to interstitial sites, resulted in the decrease of the concentration of conduction electron with increasing Mn mol%. While Eq. (4) or (5) is inhibited by Mn²⁺ ions in the high-temperature region, the formation of oxygen vacancy in In₂O₃ can be increased by Mn²⁺ ions, which means that the concentration of adsorption site (V_o) for O₂ can be increased. Moreover, since manganese ions in higher oxidation states can be reduced to Mn²⁺ at the reaction temperatures, the concentration of Mn²⁺ in the Mn-doped catalyst can be more increased during the reaction, giving rise to the increase of the concentration of oxygen vacancy.

As shown in Table 1, the 9.8 mol% Mn/In₂O₃ catalyst shows a C₂ selectivity in the methane coupling reaction. The XRD analysis in Figure 1 shows that Mn₃O₄ phase is rich on the surface of 9.8 mol% Mn/In₂O₃. The results enable us to consider that the contribution of Mn₃O₄ phase existing on the surface of catalyst to the production of C₂ hydrocarbons cannot be excluded. However, the C₂ yield of 9.8 mol% Mn/In₂O₃ catalyst is much lower than that of 5.1 mol% Mn-doped In₂O₃ catalyst as in Table 1. Therefore, it is obvious that in the present catalysts, the Mn-doping effect on the production of C₂ hydrocarbons is more significant compared to the effect by surface manganese oxide. Consequently, the

concentration of oxygen vacancy in In_2O_3 at higher temperatures can be controlled by Mn-doping, gaseous oxygen is chemisorbed on oxygen vacancy, and the adsorbed O^- selectively activates CH_4 . Methane is activated *via* abstraction of a hydrogen atom at O^- (ads) and then OH^- (ads) ions are formed on the surface of catalyst. The OH^- (ads) ions are desorbed as a form of H_2O in gas phase remaining oxygen vacancy on the surface. The resultant methyl radicals may remain attached to the surface of catalyst where coupling of methyl radicals takes place or be released into the gas phase where methyl radicals are coupled. The methyl radicals can be deeply oxidized to carbon oxides by the reaction with dioxygen in the gas phase or on the surface of the catalyst.

Acknowledgment. We are grateful to the Korea Science and Engineering Foundation for financial support (No. 921-0300-008-1).

References

- Keller, G. E.; Bhasin, M. M. *J. Catal.* **1982**, *73*, 9.
- Carreiro, J. A. S. P.; Baerns, M. *J. Catal.* **1989**, *117*, 396.
- Matsuda, T.; Minami, Z.; Shibata, Y.; Nagano, S.; Mirura, H.; Sugiyama, K. *J. Chem. Soc. Faraday Trans. I* **1986**, *82*, 1357.
- Ambigues, P.; Techner, S. J. *Discuss. Faraday Soc.* **1966**, *41*, 362.
- Schmacher, L. C.; Afara, S. M.; Dignam, M. J. *J. Electrochem. Soc.* **1986**, *133*, 716.
- Laser, D. *J. Appl. Phys.* **1981**, *52*, 5179.
- Lee, S. H.; Heo, G.; Kim, K. H.; Choi, J. S. *Int. J. Chem. Kinet.* **1987**, *19*(1), 1.
- Otsuka, K.; Yasui, T.; Morikawa, A. *J. Chem. Soc., Faraday Trans. I* **1982**, *78*, 3281.
- Brenet, J. *Bull. Soc. Chim. Fr.* **1987**, *1*, 9.
- Runyan, W. R. In *Semiconductor Measurements and Instrumentation*; McGraw-Hill: New York, 1975, p 65.
- Oku, M.; Hirokawa, K.; Ikeda, S. *J. Elect. Spect. Rela. Phenom.* **1975**, *7*, 465.
- Barr, T. L.; Liu, Y. L. *J. Phys. Chem. Solids* **1989**, *50*, 657.
- De Wit, J. H. W.; Unen, V.; Lahey, M. *J. Phys. Chem. Solids* **1977**, *38*, 819.
- McCan, J. F.; Bockris, J. O. M. *J. Electrochem. Soc.* **1981**, *128*, 1719.
- Li, C.; Domen, K.; Maruya, K.; Onishi, T. *J. Am. Chem. Soc.* **1989**, *111*, 7683.
- Li, O.; Xin, Q. *J. Phys. Chem.* **1992**, *96*, 7714.
- Haber, J.; Witko, M. *Acc. Chem. Res.* **1981**, *14*, 1.
- Lin, C.-H.; Ito, T.; Wang, J.-X.; Lunsford, J. H. *J. Am. Chem. Soc.* **1987**, *109*, 4808.
- Driscoll, D. J.; Martir, W.; Wang, J.-X.; Lunsford, J. H. *J. Am. Chem. Soc.* **1985**, *107*, 58.
- Lane, G. S.; Miro, E.; Wolf, E. E. *J. Catal.* **1989**, *119*, 161.
- Borve, K. J.; Petterson, L. G. M. *J. Phys. Chem.* **1991**, *95*, 7401.
- Burch, R.; Chalker, S.; Squire, G. D.; Tsang, S. C. *J. Chem. Soc. Faraday Trans.* **1990**, *86*, 1607.

Synthesis of β,γ -Unsaturated Ketones through Ligand-Promoted Hydroiminoacylation of Dienes by Rh

Chul-Ho Jun*, Bon-Tak Koo[†], Jung-Bu Kang[‡], and Keun-Jae Kim[‡]

Department of Chemistry, Yonsei University, Seoul 120-749, Korea

[†]*Agency for Defense Development, Yuseong P.O. Box 35, Taejeon 305-600, Korea*

[‡]*Department of Chemistry, Hannam University, Taejeon 300-791, Korea*

Received July 27, 1994

Chlorobis(isoprene)rhodium(I) (**3**), prepared by olefin-exchange reaction of chlorobis(cyclooctene)rhodium dimer (**2**) with isoprene, reacted with benzaldimine **4** to give iminoacylrhodium(III) η^3 -1,2-dimethylallyl complex **6**. Ligand-promoted reductive elimination of **6** by pyridine and $\text{P}(\text{OMe})_3$ produced β,γ -unsaturated ketimine **8**, which was readily hydrolyzed to give β,γ -unsaturated ketone **9**. Other methyl branched dienes such as 2,3-dimethylbutadiene, 3-methyl-1,3-pentadiene, 2-methyl-1,3-pentadiene, 2,4-dimethyl-1,3-pentadiene, 3-methyl-1,4-pentadiene and 2-methyl-1,4-pentadiene, were applied the synthesis of β,γ -unsaturated ketones. In case of 2,4-dimethyl-1,3-pentadiene, only γ,δ -unsaturated ketone **25**, 1,2-addition product, was obtained, maybe due to the mono-olefin coordination.

Introduction

The activation of the C-H bond by transition metal complexes is one of current interests in organometallic chemistry.¹ Especially the aldehydic C-H bond can be readily cleaved by transition metals such as Wilkinson's complex. Subse-

quent decarbonylation of the acylmetal hydride and reductive elimination of the resulting alkylmetal hydride gives alkane.² This decarbonylation can be prevented through cyclometallation due to the formation of stable 5-membered ring metallacycle as an intermediate.³ One of good substrates is 8-quinolinecarboxaldehyde, which is reacted with Rh(I) to give acyl-